Journal of Integrative Neuroscience

J. Integr. Neurosci. **2022**; 21(4): 109
https://doi.org/10.31083/j.jin2104109

Original Research

Panaxydol Derived from *Panax notoginseng* Promotes Nerve Regeneration after Sciatic Nerve Transection in Rats

Yueming Wang[1,2,3,†], Jianwen Li[4,5,†], Yan Wo[3,*], Zhengrong Zhou[1,2,6,*]

[1]Department of Radiology, Fudan University Shanghai Cancer Center, 200032 Shanghai, China
[2]Department of Oncology, Shanghai Medical College, Fudan University, 200032 Shanghai, China
[3]Department of Anatomy and Physiology, Shanghai Jiao Tong University School of Medicine, 200025 Shanghai, China
[4]Department of Urology, Dushu Lake Hospital Affiliated to Soochow University, 215100 Suzhou, Jiangsu, China
[5]Dushu Lake Branch of The First Affiliated Hospital of Soochow University, 215100 Suzhou, Jiangsu, China
[6]Department of Radiology, Minhang Branch of Fudan University Shanghai Cancer Center, 200032 Shanghai, China
*Correspondence: woyansh@163.com (Yan Wo); zhouzr_16@163.com (Zhengrong Zhou)
[†]These authors contributed equally.
Academic Editor: Francois Roman
Submitted: 30 December 2021 Revised: 22 March 2022 Accepted: 1 April 2022 Published: 7 June 2022

Abstract

Background: Peripheral nerve regeneration is a coordinated process of Schwann cell (SC) reprogramming and intrinsic neuronal growth program activation. Panaxydol (PND) is a strong biologically active traditional Chinese medicine monomer extracted from *Panax notoginseng* rhizomes. *In vitro*, PND protects neurons and SCs from injury and stimulates the expression and secretion of neurotrophic factors (NTFs) by SCs. We hypothesized that PND may also promote peripheral nerve regeneration in adult animals. **Methods**: PND (10 mg/kg body weight) was injected intraperitoneally into the Sprague–Dawley (SD) rats for two consecutive weeks after sciatic nerve transection. The morphology of the repaired sciatic nerve was evaluated after 16 weeks, and sensory and motor function recovery was evaluated using functional and behavioral techniques. **Results**: PND was biologically safe at an injection dose of 10 mg/kg/day. After 14 days, it significantly increased the myelination of regenerated nerve fibers, and promoted sensory and motor function recovery. In the early stage of injury, PND significantly upregulated the mRNA expression of brain-derived neurotrophic factor (BDNF) and its receptors in distal injured nerves, which may represent a possible mechanism by which PND promotes nerve regeneration *in vivo*. **Conclusions**: Our study demonstrated that PND leads to sensory and motor recovery in a sciatic nerve transection model rat. Furthermore, we showed that BDNF mRNA level was significantly increased in the injured distal nerve, potentially contributing to the functional recovery. Further research is warrantied to examine whether direct injection is a more efficient method to increase BDNF expression compared to an exogenous BDNF administration.

Keywords: biochemical pharmacology; panaxydol (PND); traditional Chinese medicine; peripheral nerve regeneration; Schwann cells; nerve growth factor; BDNF

1. Introduction

Peripheral nerve injury (PNI) is one of the most common neurosurgical diseases encountered in the clinical practice [1]. PNI is caused by the effects of direct or indirect externaly applied mechanic injuries, such as crushing, pulling, disconnecting, and tearing, on the peripheral nerve trunks or their branches [2]. The annual occurrence of PNI has been showing a constant rising trend, especially due to increasing harmful lifestyle implications and a better understanding of the diagnosis. In adults, a poorer peripheral nerve regeneration is observed, which easily leads to motor and sensory dysfunction and even a loss of function [3], with a high disability rate that seriously affects patients' quality of life. Deployment microsurgical procedures have improved nerve regeneration efficiency and PNI morphological recovery since their conception and deployment. In contrast, the achievement of long-term functional recovery is still vastly underdeveloped [4]. Drug therapy is an important aspect of the treatment after surgical nerve continuity reconstruction. Therefore, finding novel compounds and therapeutic strategies is of a major importance to tackle the problem of long-term side effects and full disability, in the face of currently highly inefficacious current treatment that solely target inflammation but do not promote the actual nerve repair. In addition, the currently available administration route is invasive.

The neurotrophic factor (NTF) family, which induces neuron regeneration after nerve injury [4], is the most extensively applied; however, exogenous NTFs have limited practical utility [5]. Due to the short biological half-life of NTFs, penetration of the blood-nerve barrier is difficult [6]. Due to their complex components and various targets, Chinese herbal medicines may establish a regenerative microenvironment that is more supportive of neurophysiological needs. A range of Chinese herbal drugs and ingredients have been shown to support and accelerate the peripheral nerve regeneration [7–10].

Panax notoginseng is a traditional Chinese herbal medicine (TCM) that has been used for centuries and is particularly essential in the therapeutic applications of TCM [11–13]. Panaxydol (PND), which is one of the lipophilic components extracted from *Panax notoginseng,* is a cytotoxic compound with high biological activity [14]. PND has been frequently studied for its potential antitumor activity [15,16], and researchers are increasingly interested in its favorable antioxidant and neuroprotective properties [17–20]. PND can protect primary cultured cortical neurons from NO-induced damage by regulating apoptotic and antiapoptotic proteins [21]. PND can also stimulate neurite outgrowth in PC12 cells by mimicking the effects of NGF through the cAMP-Epac1-Rap1-MEK-ERK-CREB pathway [22].

Recently, our research team reported that PND boosted the biological activity of RSC96 cells and primary SCs and promoted the expression of NTFs, such as NGF and BDNF, in SCs *in vitro* [23]. PND also shielded primary cultured neurons and SCs from hypoxic effects [24]. We confirmed that the peripheral nerve regeneration is a coordinated process that involves SC reprogramming and activation of the intrinsic neuronal growth program [6,25]. Based on our previous research, this study investigated the hypothesis that PND promotes peripheral nerve regeneration by the increase of the BDNF expression. We established a sciatic nerve transection model in adult SD rats. PND was intraperitoneally injected for two consecutive weeks. Morphology and sensory and motor function restoration of the sciatic nerve were observed and analysed.

2. Materials and Methods

2.1 Preparation of PND

Nature Standard Company, Shanghai, China, isolated and purified authentic standards of PND ((3R)-9,10-epoxy-1-ene-4,6-diyn-3-ol). Nuclear magnetic resonance (NMR) spectroscopy (^{1}H-) was used to identify PND, and the full spectral datasets were consistent with previously published values [23,26,27]. Purity was determined to be greater than 98% by high-performance liquid chromatography (HPLC). PND was stored at –20 °C in the dark and brought to room temperature before use. The solvent control solution was composed of 12% Kolliphor HS 15 (Sigma-Aldrich Inc., St. Louis, MO, USA) and 88% normal saline. Prior to injection, PND was further diluted in solvent control solution to a final concentration of 10 mg/mL. Kolliphor HS 15 has been widely used as a pharmaceutical excipient, including as a solubilizer, absorption enhancer, emulsifier, plasticizer, and vehicle for controlled drug delivery applications. According to published reports, this concentration has no discernible effect [28].

2.2 Animals and Treatment

Twenty adult SD rats (female, 7 weeks of age) were provided by the Animal Care Facility of Shanghai Jiao Tong University, School of Medicine (Shanghai, China). The rats were housed at a constant temperature (25 $\pm$ 2 °C) and were given ad libitum access to food on a 12-h light/dark cycle. All experiments were performed in accordance with the Chinese Council for Animal Care guidelines and were performed in accordance with the Animal Care Committee of Shanghai Jiao Tong University School of Medicine.

2.3 Sciatic Nerve Injury Model and Drug Treatment Protocol

Anesthesia was administered by intraperitoneal injection of sodium pentobarbital (40 mg/kg body weight, i.p.), and all animal studies were performed under aseptic conditions. Sciatic nerve transection injury was established as previously described [29]. The right sciatic nerve was exposed 1.0 cm distal to the sciatic notch and transected in the middle with sharp scissors. The lesion site was then repaired with four stitches of 9–0 microsutures (Jin Huan Co., China) through the epineurium under 20–40$\times$ magnification. The contralateral nerve was exposed but was not transected (control).

After surgery, the rats were randomly assigned to two groups: the PND group or the solvent control group. Simultaneously, all groups were given an intraperitoneal injection of the corresponding medication for two consecutive weeks at the same fixed time. Rats in the PND group received PND (10 mg/kg) daily, whereas rats in the control group received the same volume of solvent daily. Then, the rats were randomly divided into two separate experiments, as shown in Fig. 1; in experiment 1, n = 3 per group per timepoint, while in experiment 2, n = 4 per group.

2.4 Real-Time PCR

The mRNA levels of BDNF, NGF, tropomyosin-related kinase B (TrkB), and p75 neurotrophin receptor (p75NTR) in the injured distal nerve were examined by real-time PCR one and two weeks after surgery. A 1.0-cm-long section of the sciatic nerve on the distal end of the lesion was isolated and removed from anesthetized animals of both groups.

Total RNA was extracted using TRIzol (15596-018, Invitrogen, Carlsbad, CA, USA), and 2 μg of total RNA was reverse transcribed using the PrimeScript RT Reagent Kit (Perfect Real Time, DRR037A, TaKaRa Biotechnology, Kusatsu, Japan) according to the manufacturer's instructions. The mRNA levels of BDNF, NGF, TrkB, and p75NTR were quantitatively measured using SYBR Select Master Mix (4472908, Roche Diagnostics, Mannheim, Germany) and the Applied Biosystems Step-One Plus Real-Time PCR System (Life Technologies, Austin, TX, USA). The unregulated control glyceraldehyde 3-phosphate dehydrogenase (GAPDH) was used to normalize mRNA expression. The sequences of the forward and reverse primers are presented in Table 1. The threshold cycle (Ct) was calculated using the second-derivative maximum method. The

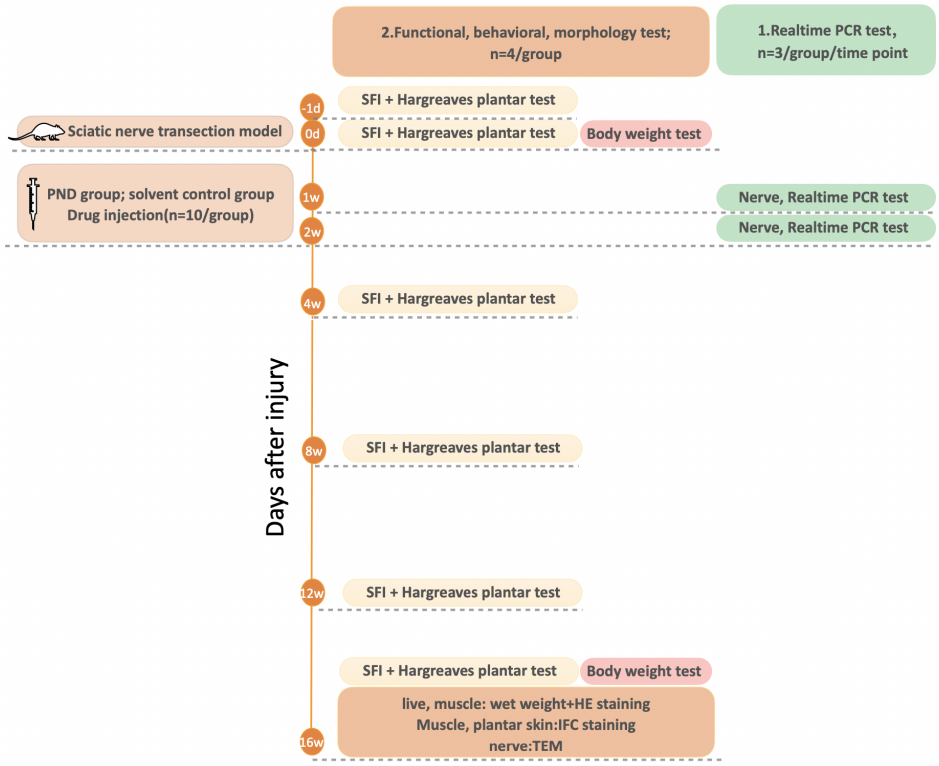

Fig. 1. Schematic diagram of the experimental procedure. On day 0, sciatic nerve transection was performed in all rats (n = 20). Following injury, the rats were randomly assigned to two groups: the PND group or the solvent control group (n = 10/group). All groups received an intraperitoneal injection of the corresponding medication for two consecutive weeks. Rats in the control group received 0.5 mL solvent daily, whereas rats in the PND group received 0.5 mL PND (10 mg/kg) daily. Then, in experiment 1, the rats were sacrificed at the indicated time points for the sampling of nerve tissues for real-time PCR (n = 3/group) analyses. In experiment 2, the walking track analysis (for evaluating motor function) along with the Hargreaves plantar test (for evaluating sensory function) were performed at the indicated time points (n = 4/group). After functional and behavioral tests were completed, the rats were weighed and sacrificed for the sampling of liver, nerve, muscle, and plantar skin tissues at 16 weeks for H&E staining, IF staining, and transmission electron microscopy (n = 4/group).

data were analyzed using the delta-delta method. The assays were performed three times using triplicate wells. The final values are reported as the ratio to the control.

Table 1. Primer Sequences for Real-Time PCR.

Primer	Sequence
GAPDH-F	AGGGTGGTGGACCTCATGG
GAPDH-R	AGCAACTGAGGGCCTCTCTCTT
NGF-F	GTCTGGGCCCAATAAAGGCT
NGF-R	CTGTGTACGGTTCTGCCTGT
BDNF-F	GTCACAGCGGCAGATAAAAAG
BDNF-R	ATGGGATTACACTTGGTCTCGT
TrkB-F	CGACACTCAGGATTTGTATTGC
TrkB-R	ATGGTCACAGACTTCCCTTCC
p75NTR-F	AGCAGACCCATACGCAGACT
p75NTR-R	GCAGTTTCTCTACCTCCTCACG

2.5 Hargreaves Plantar Test

All behavioral experiments described below were conducted in a blinded manner in a quiet room (temperature 25 ± 1 °C) from 9 AM to 6 PM. The surgeon who performed the transection injury and the behavioral observers were different individuals. The rats were habituated to the experimental setting for three consecutive days before the start of the experiment, and the daily acclimatization time was calculated to be the duration of the experiment.

The Hargreaves plantar test (Yuyan, Shanghai, China) was used to assess the injured hindlimb's heat sensitivities and sensory functional recovery of rats (n = 4/group). The tests were performed at six time points: 1 day before surgery and 1 day, 4 weeks, 8 weeks, 12 weeks, and 16 weeks after surgery. The light intensity of the selected heat source beam was IR = 75%, and the upper limit of the pain threshold latency was set to 20.1 s to avoid scalding the rat's foot. Briefly, each rat was placed on the glass plate of the pain tester, separated by a special transparent plastic

box, and allowed to adapt for more than 30 min. The light source of the tester was switched on while ensuring that the heat source beam emitted by the transmitter aim was located outside of the middle part of the sole of the foot. The time interval between initial activation and paw withdrawal in response was recorded automatically. Heat stimulation was stopped to prevent thermal injury if the animals did not withdraw their paws after 20 s. The test was repeated three times for each rat (15-min intervals were included between tests), and the average value of each measurement was recorded to represent the thermal pain threshold.

2.6 Walking Track Analysis

The recovery of motor function in rats (n = 4/group) was examined by walking track analysis at six time points: 1 day before surgery and 1 day, 4 weeks, 8 weeks, 12 weeks, and 16 weeks after surgery. The rats were habituated to the experimental setting for three consecutive days before the start of the experiment, and the daily acclimatization time was calculated to be the duration of the experiment.

Then, the sciatic functional index (SFI) was calculated as previously described [30,31]. Briefly, the rats were trained to walk across a custom-made walking box (100 cm long, 12 cm wide, and 10 cm high) leading to a darkened box. White paper (12 cm × 100 cm) lined the bottom of the track. The rat's hind paws were dipped in red dye before it walked the track at each timepoint. Each rat was then allowed to walk the track three or four times until five measurable footprints were collected. Then, the SFI was measured and calculated using the following formula:

SFI = (–38.3 × (EPL-NPL)/NPL) + (109.5 × (ETS-NTS)/NTS) + (13.3 × (EIT-NIT)/NIT) – 8.8

PL: the distance from the heel to the top of the third toe;

IT (intermediary toe spread): the distance from the second to the fourth toe;

TS (toe spread): the distance between the first and the fifth toe.

The normal print length (NPL), normal toe spread (NTS), and normal intermediary toe spread (NIT) represent the PL, IT, and TS recorded from the uninjured, normal foot; experimental print length (EPL), experimental toe spread (ETS), and experimental intermediary toe spread (EIT) represent the PL, IT, and TS recorded from the paired, injured, experimental foot, respectively. An SFI value of approximately 0 indicates full recovery, whereas an SFI value of approximately 100 represents complete dysfunction.

2.7 Wet Weight and H&E Staining of the Liver and Gastrocnemius Muscle

After functional and behavioral tests were completed, the rats (n = 4/group) were weighed and sacrificed carefully 16 weeks after surgery. Organs and tissues including the liver, injured nerve, plantar skin, and gastrocnemius muscles were collected from the injured and uninjured sides. The livers and gastrocnemius muscles from the injured and uninjured sides were then weighed. Blood vessels and the deep fascia covering the surfaces of the liver and muscle were removed and discarded before weighing. The following equation was used to determine the rate of body weight gain, liver hepatosomatic, and recovery rate of the gastrocnemius muscles:

Rate of body weight gain = (final body weight-initial body weight)/initial body weight

Hepatosomatic index = wet weight of the liver/final body weight

The recovery rate of the gastrocnemius muscle = wet weight of the injured muscle/wet weight of the uninjured muscle

After weighing, the liver and mid belly of the gastrocnemius muscle specimens were cut into small pieces, fixed in 4% paraformaldehyde/PBS, and dehydrated in a graded series of ethanol. Then, the samples were paraffin-embedded, cut into 5-μm-thick sections, and stained with H&E. The H&E-stained fibers were analyzed in a blinded manner using ImageJ software (NIH, Bethesda, MD, USA). The fibers were manually evaluated, and the program was used to calculate the cross-sectional area of each fiber. The quantitative study was conducted using the cross-sectional area of muscle fibers as the unit of measurement.

2.8 Neuromorphological Analysis

After functional and behavioral tests were completed, a 0.5-cm-long piece of the sciatic nerve at the 1 cm distal end of the lesion was separated and removed from the rats (n = 4/group). The nerves were sliced into 5-μm-thick cross-sections and stained with toluidine blue. We assessed the morphology in cross-sections of nerve to measure and calculate the diameter, myelin thickness, and g-ratio of the myelinated nerve fibers of the distal nerve stump.

Myelin staining with toluidine blue: The segments were stained with 1% toluidine blue at room temperature for 30 min, washed gently in water, and consecutively soaked in 95% ethanol and 100% ethanol for 2–3 s. Images were acquired at 400× magnification using a dissecting microscope (M205FA, Leica, Wetzlar, Germany). The axon and fiber diameters were measured using ImageJ software (NIH, Bethesda, MD, USA). Myelin thickness and g-ratio were calculated as follows: myelin thickness = (fiber diameter – axon diameter)/2; g-ratio = axon diameter/fiber diameter.

Transmission electron microscopy: Sections of regenerated nerves were fixed in precooled 2.5% glutaraldehyde for 3 h followed by postfixation in a 1% osmium tetroxide solution for 1 h, washed, dehydrated, embedded in Epon 812 epoxy resin, cut into ultrathin sections at 60 nm, and stained with lead citrate and uranyl acetate. The stained sections were observed under a transmission electron microscope (JEM-1200, JEOL Ltd., Tokyo, Japan).

2.9 Immunohistochemical Staining

Nerve, skin, and muscle were postfixed in 4% paraformaldehyde/PBS overnight after which tissues were incubated in 30% sucrose/PBS overnight for dehydration. Then, the tissues were frozen in Tissue-Tek O.C.T. (4583, Sakura Finetek, CA, USA). Then, 10-μm-thick specimens were sectioned using a cryostat (Thermo Fisher Scientific, Austin, TX, USA), mounted on glass slides, and dried for future immunostaining. The slides were washed three times in 0.01 M PBS for 5 min, blocked with 10% NGS/0.1% Triton X-100 in 0.1 M PBS for 1 h at room temperature, and incubated overnight at 4 °C with primary antibodies (PGP 9.5, nerve terminals marker, Abcam ab8189, 1:500). After three 10-min washes in PBS, the slides were incubated with CY3-conjugated goat anti-mouse IgG (Abcam, ab97053, 1:100) for 1 h at 37 °C and rinsed three times in PBS for 5 min each time. To stain the end plate, the slides containing muscle tissue were incubated with FITC-conjugated bungarotoxin (Life Technologies, B-13422, 1:1000) for an additional 5 h at 37 °C, followed by three 10-min washes in PBS. Gel/Mount aqueous mounting media (Biomeda Corp., Foster, CA, USA) was used to mount the coverslips, after which slides were viewed under a digital fluorescence microscope (M205FA, Leica, Welzlar, Germany). Five random visual fields of the gastrocnemius muscle sections at 100× magnification were selected, and the numbers of end plates in 10 sections from each reinnervated muscle specimen were counted. Only end plates double-stained with both bungarotoxin and PGP9.5 were counted.

2.10 Statistical Analysis

Statistical analyses were performed using GraphPad Software (GraphPad 9, La Jolla, CA, USA). The data are presented as the means ± standard deviations. One-way analysis of variance followed by the Student-Newman–Keuls post hoc test was used to compare the PND and solvent control groups or other groups as indicated. A p value < 0.05 was considered statistically significant.

3. Results

3.1 Hepatic Toxicity and Histopathology Evaluation of PND

The toxicity and safety of traditional Chinese medicine have garnered increased attention in recent decades. The liver is the primary site of drug transformation and metabolism and is also the main target organ for drug toxicity [32–34]. To evaluate the side effects and toxicity of PND, we investigated body weight gain, hepatosomatic index, and liver histopathologic characteristics of both groups of rats. Rats in both groups survived the experiment without obvious ascites, emaciation, or self-mutilation. Each rat gained approximately 40–52 g of body weight in both groups, and no significant difference was observed in the rate of body weight gain or in the hepatosomatic index between the two groups (Fig. 2C; n = 4, $p > 0.05$). As shown in Fig. 2, 16 weeks after nerve transection, H&E staining and light microscopy revealed an intact structure of liver lobules in rats of both groups; liver plates were neatly arranged, and no obvious morphological changes, such as swelling, necrosis, or inflammatory cell infiltration, were observed. PND did not cause pathological changes in the liver when administered at a dose of 10 mg/kg/d for two consecutive weeks.

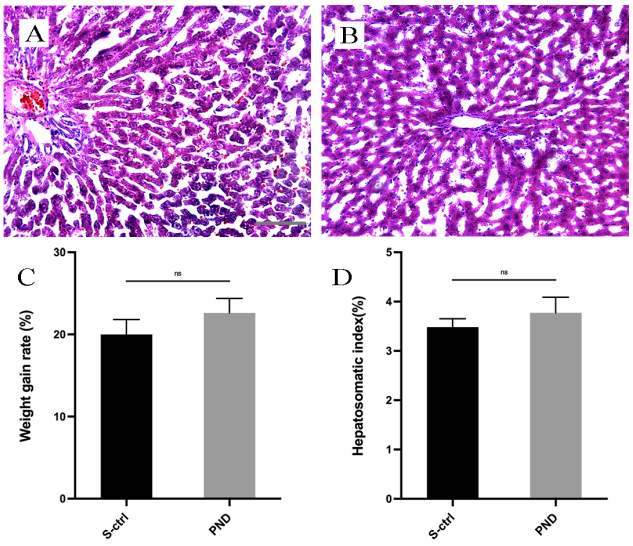

Fig. 2. H&E staining and histological analysis of the liver in each group. Representative light micrographs of H&E-stained liver sections from the solvent control group (A) and the PND group (B) 16 weeks after surgery. The rate of weight gain in each group is shown in panel (C). The hepatosomatic index in each group is shown in panel (D). All data are presented as the means ± standard deviations. $p > 0.05$ for comparisons with the solvent control group. Scale bar: 100 μm.

3.2 Distal Axonal Regeneration and Myelination Analysis

After 16 weeks, cross-sections of tissue 1 cm distal to the injury were obtained for the morphologic analysis of the ingrowth of regenerated nerve fibers. SCs surround regenerated nerve processes to reform myelin sheaths or unmyelinated fibers, which provides a structural basis for the subsequent recovery of nerve conduction function [35]. Along with the density of regenerated nerve fibers, the thickness of the myelin sheath, the diameter of nerve fibers, and the g-ratio all serve as important indicators of regenerated nerve fiber maturation. Toluidine blue staining was used to assess distal nerve fiber formation and myelination. The results of toluidine blue staining at the distal end of the injury are shown in Fig. 3A,B. Sixteen weeks after sciatic nerve injury, both groups demonstrated significant regeneration of nerve fibers at the distal end of the injury, with some fibers forming myelin sheaths. Additionally, the average fiber diameter and myelin sheath thickness were signif-

icantly greater in the PND group than in the solvent control group (Fig. 3C; n = 4, $p < 0.05$). However, PND treatment did not significantly improve the degree of myelination (g-ratio) after injury compared with the solvent control (Fig. 3C; n = 4, $p > 0.05$). The ultrastructure of regenerated fibers was revealed by transmission electron microscopy. The morphological appearance and mature structure of the regenerated axons in the PND group were superior to those in the control group (Fig. 3D–G).

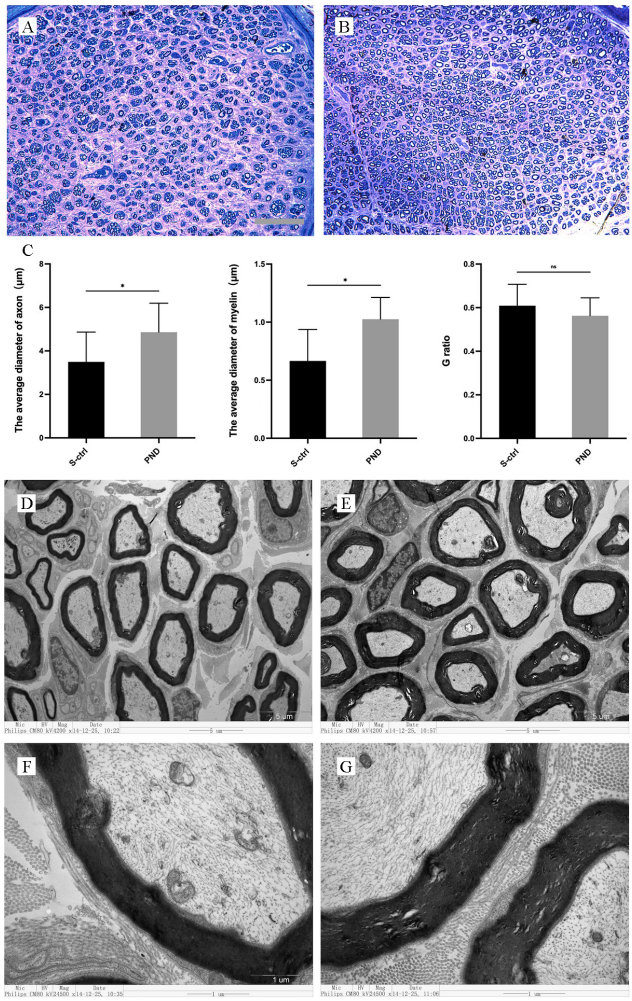

Fig. 3. Morphological appearance and morphometric assessments of regenerated and myelinated nerves in each group. Representative images show toluidine blue staining of regenerated axons (A,B) 1 cm distal to the injury site in the solvent control group (A) and PND group (B) 16 weeks after injury. A, B: scale bar: 50 μm. Morphometric assessments of regenerated and myelinated nerves (C). All data are presented as the means ± standard deviations. *$p < 0.05$ compared with the solvent control group. Representative electron micrographs of regenerated axons (D,E) and the myelin sheath (F,G) 1 cm distal to the injury in the solvent control group (D,F) and PND group (E,G) 16 weeks after surgery. D,E: scale bar: 5 μm; F,G: scale bar: 1 μm.

3.3 Recovery of Gastrocnemius Muscle Fibers

By collecting, weighing, and staining the gastrocnemius muscle with H&E 16 weeks after nerve injury, we assessed the healing of target organs following treatment.

As illustrated in Fig. 4A,B, gastrocnemius muscle atrophy was detected in both groups of rats following denervation.

Fig. 4 illustrates the morphometric evaluations (C). The gastrocnemius recovery rate (the ratio of muscle wet weight on the injured side to that on the contralateral side) and the area of a single myocyte in the control group were both lower than those in the PND group (Fig. 4C; n = 4, $p < 0.05$), which implies that muscle atrophy was more severe in the control group.

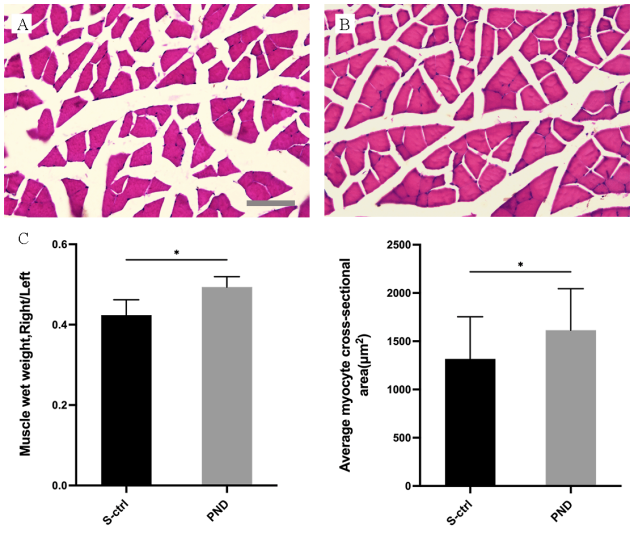

Fig. 4. Morphological appearance and morphometric assessments of gastrocnemius muscle fiber recovery in each group. Representative light micrographs of H&E-stained transverse sections of the gastrocnemius muscle (A,B) from rats in the solvent control group (A) and the PND group (B) 16 weeks after injury. A, B: scale bar: 100 μm. The gastrocnemius recovery rate and the area of a single myocyte in the control group were both lower than those in the PND group (C). All data are presented as the means ± standard deviations. *$p < 0.05$ for comparisons with the solvent control group.

3.4 Degree of Target Organ Reinnervation

To evaluate the target organ condition, immunofluorescence (IF) staining was used to detect the reinnervation of muscle and skin by sciatic nerve terminals in the two groups 16 weeks after injury. Neuromuscular junction staining is shown in Fig. 5A,B. Double staining and colocalization of markers of the end plate and nerve terminals was seen in both groups, which indicates effective reinnervation. The number of reinnervated end plates in each visual field in the PND group was not significantly different

from that in the control group (Fig. 5C; n = 4, $p < 0.05$).

Both groups displayed regenerated nerve fiber ingrowth in the plantar skin, as illustrated in Fig. 5D,E. Imaging analysis revealed no statistically significant difference in nerve fiber length per unit area between the PND and control groups (Fig. 5F; n = 4, $p < 0.05$).

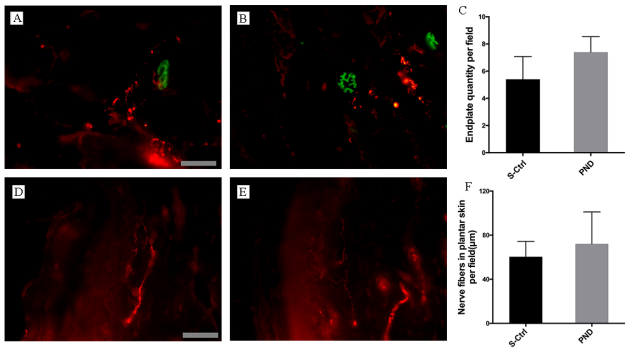

Fig. 5. Morphological appearance and morphometric assessments of reinnervated muscle and skin in each group. Representative images of IF staining for PGP 9.5 (red) and FITC-conjugated α-bungarotoxin (green) in reinnervated muscle (A,B) and skin (D,E) 1 cm distal to the injury in the solvent control group (A,D) and PND group (B,E) 16 weeks after injury. (A,B,D,E): scale bar: 50 μm. Partial neuromuscular junctions (NMJs) were colocalized with PGP 9.5-positive fibers. Morphometric assessments of reinnervated muscle (C) and skin (F). All data are presented as the means $\pm$ standard deviations. $p > 0.05$ for comparisons with solvent control groups.

3.5 Recovery of Sciatic Nerve Sensory Function

The Hargreaves plantar test data were collected every four weeks after injury and revealed that sensory functional recovery was complete in both groups. As illustrated in Fig. 6, the plantar skin of rats gradually recovered sensitivity to heat and pain. After approximately four weeks for the PND group and after approximately eight weeks for the control group, the rats recovered to near-normal levels of sensory function (Fig. 6; n = 4, * $p < 0.05$, compared with before injury). The PND group recovered sensory function more quickly than the control group. Additionally, the PND group experienced greater sensory recovery than the control group after four weeks (Fig. 6; n = 4, $^{\#}$ $p < 0.05$).

3.6 The Reestablishment of Motor Function in the Sciatic Nerve

A greater SFI suggests stronger sciatic nerve function. The return to preinjury SFI levels indicates complete recovery of hindlimb motor coordination and function, including that of the most distal paw muscles. Every four weeks, animals in both groups were given an SFI test to measure the recovery of motor function of the sciatic nerve. Statistical analysis of SFI data indicated that motor functional recovery was only partially achieved in both groups. SFI values remained low compared with preinjury levels at all time intervals evaluated up to 16 weeks (Fig. 6; n = 4, * $p < 0.05$, compared with values before injury), which demonstrates poor recovery of motor function. However, at 8, 12, and 16 weeks after injury, the SFI values in the PND group were substantially higher than those in the control group (Fig. 6; n = 4, $^{\#}p < 0.05$), which shows that rats in the PND group experienced greater motor functional recovery.

3.7 The mRNA Expression of NTF and its Receptors at the Injured Sites

NGF and BDNF mRNA levels in the injured distal nerve were examined using real-time PCR one and two weeks after injury. As shown in Fig. 7, NGF mRNA levels were similar in the PND group and control group at one and two weeks after surgery (n = 3, $p > 0.05$). At one and two weeks after surgery, the BDNF mRNA levels in the PND group were 1.57-fold and 1.89-fold higher, respectively, than those in the control group (n = 3, $p < 0.05$). The functions of BDNF are mediated by its high-affinity receptor (TrkB) and low-affinity receptor (p75NTR). Additionally, we used real-time PCR to determine the mRNA levels of p75NTR and TrkB in the injured distal nerve one and two weeks after injury. The expression levels of p75NTR and TrkB mRNA in the PND group were 1.99-fold and 2.09-fold greater, respectively, than those in the control group at one week (n = 3, $p < 0.05$). In addition, the expression of p75NTR mRNA remained high in the PND group (1.90-fold higher than that of the control group) at two weeks (n = 3, $p < 0.05$).

4. Discussion

The PNS is mainly composed of nerve processes and glial cells (SCs) [36]. SCs are myelinated glial cells unique to the PNS that play a key role in regeneration after nerve injury [37]. After PNS injury, both myelinating and non-myelinating SCs undergo substantial reprogramming to facilitate and direct axonal growth [6]. SCs divide and proliferate, provide appropriate numbers of cells and a basement membrane skeleton, form a Büngner band, and provide mechanical growth channels for regenerating axons [38]. They also secrete a variety of NTFs and nerve cell adhesion factors and provide an active surface to promote the adherent growth of axons. In addition, SCs surround regenerated nerve processes to reform myelin sheaths or unmyelinated fibers, which provides a structural basis for the subsequent recovery of nerve conduction function [35].

After PNI, the use of microsurgical techniques sufficiently restores the continuity of injured nerve fibers and is an important component of subsequent clinical treatment. Drug treatment provides a good microenvironment for nerve regeneration. The most common treatments related to the NTF family have been shown to promote re-

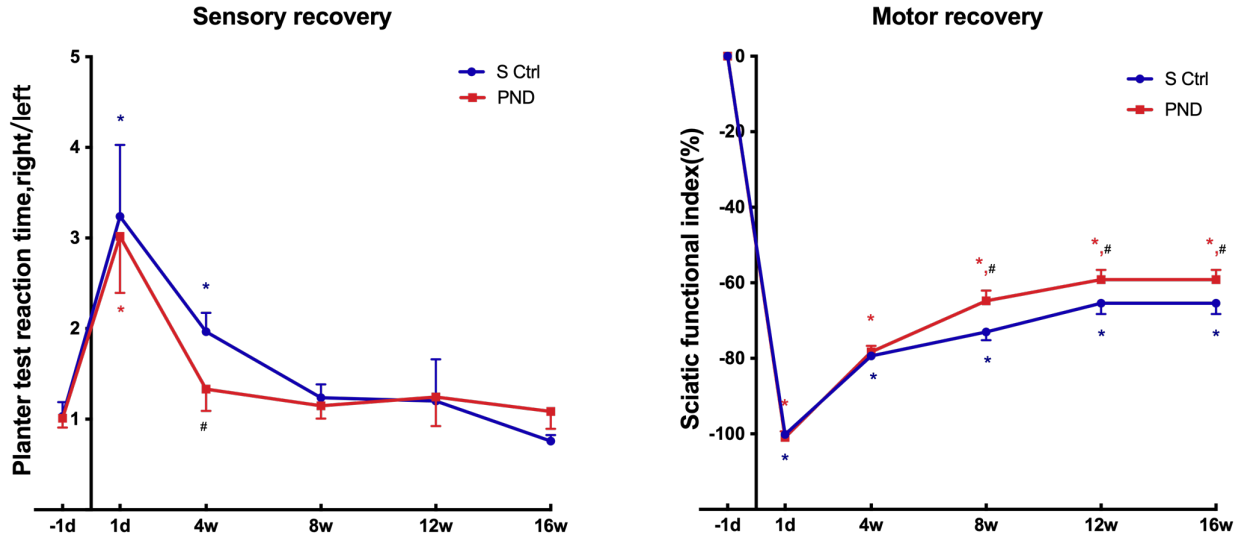

Fig. 6. Motor and sensory functional recovery in each group. The SFI (a score of –100 and below corresponds to total paralysis, whereas uninjured animals typically have a score of –8.8 or higher) and plantar test reaction time rate tested 1 day before injury and 1 day, 4 weeks, 8 weeks, 12 weeks, and 16 weeks after injury. $^{*}p < 0.05$ for comparisons with values before injury. $^{\#}p < 0.05$ for comparisons with the solvent control group at paired time points.

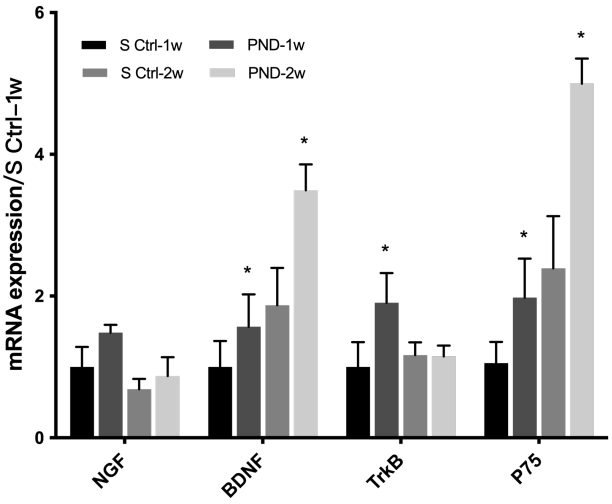

Fig. 7. Expression of neurotrophic factors and their receptors in each group one and two weeks after injury. The mRNA levels of NGF, BDNF, and their receptors TrkB and p75NTR at the injured sites were determined in the solvent control and PND groups at one and two weeks after injury. Each test was repeated three times. All data are presented as the means ± standard deviations. $^{*}p < 0.05$ for comparisons with the solvent control group at the same timepoint after injury.

generation after nerve injury [39]. However, due to their short biological half-life, the clinical application of NTFs is still limited due to enzymolysis, inactivation, antigenic immune reactions, and the limited effect of single drugs [40]. However, a variety of Chinese herbal medicines and compounds have been shown to promote nerve repair and regeneration after injury [7,10]. Chinese herbal medicines are characterized by complex components, a wide range of actions, and many targets. Notably, the complexity of Chinese herbal formulas and single herbal medicines results in low specificity, low efficacy, and the occurrence of side effects, particularly serious liver damage. Furthermore, due to the complexity of the components, the molecular biological basis and pharmacological mechanisms of action have not been clarified. In recent years, the screening and analysis of single active ingredients in herbal medicines have led to novel methods for pharmacological research on Chinese herbal medicine and are important for identifying small-molecule compounds with specific targets.

As a traditional medicine used in China, *Panax notoginseng* has been shown to possess various biological properties related to immune defense, antioxidant capability [41–43], improvements in blood pressure [11–13], and neurotrophic functions [44–47], and its medicinal value has been recognized worldwide. PND is a fat-soluble component isolated from the rhizome of *Panax notoginseng* [48]. PND exhibits strong biological activity due to a reactive oxygen atom in its structure [49]. Our *in vitro* studies have shown the protective and nutritional effects of PND on cultured neurons and SCs [23,24]. This study further confirmed the effect of PND on peripheral nerve repair *in vivo* and further explored the underlying mechanisms.

After PNI, the diameter and thickness of the myelin sheath of myelinated nerve fibers were significantly greater in the PND group than in the control group, which implies that PND promotes nerve fiber regeneration and SC

myelination. The Hargreaves plantar test indicated that sensory function recovered more rapidly in the PND group, although no significant difference was observed in the length of the reinnervated nerve growing into the plantar skin between the PND and control groups at 16 weeks. For motor nerve target muscles, neither the area of nerve fiber growth into the gastrocnemius nor the number of NMJs in the muscle showed significant differences between the PND treatment group and the control group. However, gastrocnemius atrophy was less severe in PND rats than in control rats. The SFI is the most frequently used indicator of motor function recovery following sciatic nerve injury and is determined by a walking trajectory analysis. The SFI has a high degree of sensitivity and accuracy and clearly demonstrates the direct relationship between hind limb muscle function and footprints [50,51]. In this study, the SFI indicated that the PND group recovered motor function slightly more quickly than the control group at week 12; however, recovery of motor function in both the PND and control groups remained suboptimal at 16 weeks.

After PNI, the recovery of sensory and motor functions is usually unequal [52]. Sakuma *et al*. [31] reported that sensory function was fully recovered in model rats by day 55 after transection injury; in marked contrast, the SFI remained at the lowest score even at day 90. This finding is also consistent with our results. In clinical practice, for example, the protective sensation in the fingers is restored in 90% of patients with a brachial plexus injury even though recovery of the thenar muscle is very limited, and the sensory axons can reinnervate even the most distal skin areas [53]. However, many studies have shown that even if regenerated nerve axons successfully reach the target muscle after injury and form complete anatomical NMJs with no abnormal ultrastructure, these NMJs do not normally activate the muscles, and recovery of motor function is still unsatisfactory. Researchers have proposed that this observation is due to the loss of motor function caused by the failure of chemical synapse reconstruction in the target muscle after long-term denervation. Nerve regeneration may require active nutritional signals, such as NTFs or synaptic collagen, from muscles to complete chemical synaptic reconstruction [54]. Therefore, we postulate that the condition of the motor end plate does not reflect the state of motor function recovery; the nutritional status of the target muscle may affect nerve regeneration and indirectly reflect the degree of motor function recovery. Gastrocnemius atrophy was significantly lower in rats in the PND group than in rats in the control group, which may explain the relatively better recovery of motor function in the PND rats.

By examining the NGF and BDNF mRNA levels in distal nerves in the early stage of injury (one and two weeks), we investigated a possible mechanism by which PND promotes peripheral nerve regeneration. PND upregulated BDNF mRNA expression in distal nerves, and this trend is also consistent with the previous *in vitro* experimental results reported by our team. To date, many studies have elucidated the important role of NTFs, including NGF and BDNF, in the process of peripheral nerve repair [55–57]. NGF is one of the most important bioactive molecules in the PNS, as it affects neuronal survival and differentiation. After PNI, NGF protects injured neurons and promotes neurite regeneration. The level of NGF produced by distal SCs peaks within 24 h of nerve transection and remains at 5–10 times the normal level for at least two weeks following axon transection. BDNF protects damaged neurons and promotes the growth of regenerated nerves [57]. Gordon and colleagues also found that BDNF levels are closely related to the selectivity of motor nerve regeneration [58]. In summary, after PNI, the increased expression of NGF and BDNF, which protect injured neurons, promotes the growth of regenerated nerve processes and nourishes denervated target organs, thereby improving the efficiency of nerve regeneration through various functions. NTF can be used as drug therapy, but usually cannot penetrate the blood-brain barrier. Whether or not this is true for PND is still unclear. Further research is needed to investigate whether and if yes, to which extent the permeability can be warranted.

In addition, the functions of BDNF are achieved through a family of high-affinity receptors (Trk family) and a low-affinity receptor (p75NTR) [59]. The expression levels of p75NTR and TrkB were upregulated in the sciatic nerve of animals in the PND group. TrkB mediates the positive neurotrophic effect of BDNF, protects damaged neurons, promotes the growth of regenerated nerves, and participates in the selective regulation of nerve regeneration. In contrast, p75NTR does not have any kinase activity [60] but rather recruits different intracellular binding proteins to activate different signaling pathways. These signaling pathways have multiple functions in different cellular environments. On the one hand, p75NTR interacts with sortilin family members to induce neuronal cell apoptosis. On the other hand, p75NTR not only directly activates survival signals but also promotes TrkB translocation and signal transduction after binding to BDNF. In addition, the myelination of BDNF depends on p75NTR, and p75NTR knockout affects myelination of the sciatic nerve during injury. In summary, PND may activate the TrkB receptor and p75NTR to initiate the positive neurotrophic effects of BDNF and promote peripheral nerve regeneration.

5. Conclusions

The main objective and scope of the study was to objectify the PND-support of peripheral nerve regeneration using a sciatic nerve transection model in adult SD rats.

We performed morphological experiments to ascertain the maturity of regenerated nerves, the number of nerve fibers reinnervating target organs, and the degree of muscle atrophy in target organs. In addition, we examined sensory and motor functions in rats by conducting functional and behavioral experiments. The nerve regeneration efficiency of

the PND group was superior to that of the solvent control group. After combining the mRNA data obtained in this study and the results of previous cell-based experiments, we speculate that PND promotes the secretion of BDNF by SCs after PNI and that BDNF initiates nerve and muscle nutritional functions by activating TrKB- and p75NTR-mediated signaling pathways. Our studies have identified the effect of PND on peripheral nerve repair *in vivo* and further explored the underlying mechanisms in nerve repair. However, the cellular and molecular mechanisms and related pathways remain unclear. Notably, a PND injection is a more easily accessible and convenient method of increasing BDNF expression than exogenous BDNF administration. Therefore, the study demonstrated that PND' bioavailability and lipophilic features provide a theoretical basis for the future clinical applications of PND. Further research is required, first on a larger number of various model organisms, follow by clinical trials. This study, however, brings major insights for this research field by demonstrating the core efficacy and efficiency of PND injections for PNI, including mechanism of action and active compounds.

Abbreviations

SC, Schwann cell; PND, panaxydol; SD rats, Sprague–Dawley rats; NTFs, neurotrophic factors; PNI, peripheral nerve injury; PNS, peripheral nervous system; BDNF, brain-derived neurotrophic factor; TCM, traditional Chinese herbal medicine; NGF, nerve growth factor; NMR, nuclear magnetic resonance; HPLC, high-performance liquid chromatography; TrkB, tropomyosin-related kinase B; p75NTR, p75 neurotrophin receptor; GAPDH, glyceraldehyde 3-phosphate dehydrogenase; SFI, sciatic functional index; PL, print length; IT, intermediary toe spread; TS, toe spread; NMJ, neuromuscular junction

Author Contributions

ZZ and YW designed the research study. YMW and JL performed the experiments. YMW analyzed the data. YMW and JL wrote the manuscript. ZZ and YW edited the manuscript. All authors contributed to editorial changes in the manuscript. All authors read and approved the final manuscript.

Ethics Approval and Consent to Participate

All experiments followed the Chinese Council for Animal Care guidelines and were in accordance with the Animal Care Committee of FuDan University (201903001S).

Acknowledgment

The authors thank Wenlong Ding from Shanghai Jiao Tong University School of Medicine for his experimental guidance and help. Ewelina Biskup assisted in the revision of the manuscript.

Funding

This research was financially supported by National Natural Science Foundation of China (No. 81672247), Shanghai Science and Technology Development Foundation (Grant No. 21ZR1436100, Grant No. 15ZR1408000 and Grant No. 18140901200).

Conflict of Interest

The authors declare no conflict of interest.

References

[1] Lu Y, Li R, Zhu J, Wu Y, Li D, Dong L, *et al*. Fibroblast growth factor 21 facilitates peripheral nerve regeneration through suppressing oxidative damage and autophagic cell death. Journal of Cellular and Molecular Medicine. 2019; 23: 497–511.

[2] Wu D, Murashov AK. Molecular mechanisms of peripheral nerve regeneration: emerging roles of microRNAs. Frontiers in Physiology. 2013; 4: 55.

[3] IJkema-Paassen J, Jansen K, Gramsbergen A, Meek MF. Transection of peripheral nerves, bridging strategies and effect evaluation. Biomaterials. 2004; 25: 1583–1592.

[4] Li R, Li D, Wu C, Ye L, Wu Y, Yuan Y, *et al*. Nerve growth factor activates autophagy in Schwann cells to enhance myelin debris clearance and to expedite nerve regeneration. Theranostics. 2020; 10: 1649–1677.

[5] Li R, Li DH, Zhang HY, Wang J, Li XK, Xiao J. Growth factors-based therapeutic strategies and their underlying signaling mechanisms for peripheral nerve regeneration. Acta Pharmacologica Sinica. 2020; 41: 1289–1300.

[6] Nocera G, Jacob C. Mechanisms of Schwann cell plasticity involved in peripheral nerve repair after injury. Cellular and Molecular Life Sciences. 2020; 77: 3977–3989.

[7] Kou Y, Wang Z, Wu Z, Zhang P, Zhang Y, Yin X, *et al*. Epimedium extract promotes peripheral nerve regeneration in rats. Evidence-Based Complementary and Alternative Medicine. 2013; 2013: 954798.

[8] Jiang X, Ma J, Wei Q, Feng X, Qiao L, Liu L, *et al*. Effect of frankincense extract on nerve recovery in the rat sciatic nerve damage model. Evidence-Based Complementary and Alternative Medicine. 2016; 2016: 3617216.

[9] Zhao Z, Li X, Li Q. Curcumin accelerates the repair of sciatic nerve injury in rats through reducing Schwann cells apoptosis and promoting myelinization. Biomedicine & Pharmacotherapy. 2017; 92: 1103–1110.

[10] Liu GM, Xu K, Li J, Luo YG. Curcumin upregulates S100 expression and improves regeneration of the sciatic nerve following its complete amputation in mice. Neural Regeneration Research. 2016; 11: 1304–1311.

[11] Pang HH, Li MY, Wang Y, Tang MK, Ma CH, Huang JM. Effect of compatible herbs on the pharmacokinetics of effective components of Panax notoginseng in Fufang Xueshuantong Capsule. Journal of Zhejiang University SCIENCE B. 2017; 18: 343–352.

[12] Tian Z, Pang H, Du S, Lu Y, Zhang L, Wu H, *et al*. Effect of Panax notoginseng saponins on the pharmacokinetics of aspirin in rats. Journal of Chromatography B. 2017; 1040: 136–143.

[13] Zhao S, Zheng MX, Chen HE, Wu CY, Wang WT. Effect of panax notoginseng saponins injection on the p38MAPK pathway in lung tissue in a rat model of hypoxic pulmonary hypertension. Chinese Journal of Integrative Medicine. 2015; 21: 147–151.

[14] Knispel N, Ostrozhenkova E, Schramek N, Huber C, Peña-

Rodríguez LM, Bonfill M, *et al*. Biosynthesis of panaxynol and panaxydol in Panax ginseng. Molecules. 2013; 18: 7686–7698.
[15] Lee JH, Leem DG, Chung KS, Kim KT, Choi SY, Lee KT. Panaxydol derived from Panax ginseng inhibits G(1) cell cycle progression in non-small cell lung cancer via upregulation of intracellular Ca^{2+} levels. Biological and Pharmaceutical Bulletin. 2018; 41: 1701–1707.
[16] Kim HS, Lim JM, Kim JY, Kim Y, Park S, Sohn J. Panaxydol, a component of Panax ginseng, induces apoptosis in cancer cells through EGFR activation and ER stress and inhibits tumor growth in mouse models. International Journal of Cancer. 2016; 138: 1432–1441.
[17] Lee D, Lee J, Vu-Huynh KL, Van Le TH, Tuoi Do TH, Hwang GS, *et al*. Protective effect of panaxynol isolated from panax vietnamensis against cisplatin-induced renal damage: *in vitro* and *in vivo* studies. Biomolecules. 2019; 9: 890.
[18] Park JY, Choi P, Kim T, Ko H, Kim HK, Kang KS, *et al*. Protective effects of processed ginseng and its active ginsenosides on cisplatin-induced nephrotoxicity: *in vitro* and *in vivo* studies. Journal of Agricultural and Food Chemistry. 2015; 63: 5964–5969.
[19] Shin IS, Kim DH, Jang EY, Kim HY, Yoo HS. Anti-fatigue properties of cultivated wild ginseng distilled extract and its active component panaxydol in rats. Journal of Pharmacopuncture. 2019; 22: 68–74.
[20] Li J, Lu K, Sun F, Tan S, Zhang X, Sheng W, *et al*. Panaxydol attenuates ferroptosis against LPS-induced acute lung injury in mice by Keap1-Nrf2/HO-1 pathway. Journal of Translational Medicine. 2021; 19: 96.
[21] Nie BM, Jiang XY, Cai JX, Fu SL, Yang LM, Lin L, *et al*. Panaxydol and panaxynol protect cultured cortical neurons against Abeta25-35-induced toxicity. Neuropharmacology. 2008; 54: 845–853.
[22] Li WP, Ma K, Jiang XY, Yang R, Lu PH, Nie BM, *et al*. Molecular mechanism of panaxydol on promoting axonal growth in PC12 cells. Neural Regeneration Research. 2018; 13: 1927–1936.
[23] He J, Ding WL, Li F, Xia R, Wang WJ, Zhu H. Panaxydol treatment enhances the biological properties of Schwann cells *in vitro*. Chemico-Biological Interactions. 2009; 177: 34–39.
[24] Zhu H, Wang WJ, Ding WL, Li F, He J. Effect of panaxydol on hypoxia-induced cell death and expression and secretion of neurotrophic factors (NTFs) in hypoxic primary cultured Schwann cells. Chemico-Biological Interactions. 2008; 174: 44–50.
[25] Namgung U. The role of Schwann cell-axon interaction in peripheral nerve regeneration. Cells, Tissues, Organs. 2014; 200: 6–12.
[26] Yeo CR, Yong JJ, Popovich DG. Isolation and characterization of bioactive polyacetylenes Panax ginseng Meyer roots. Journal of Pharmaceutical and Biomedical Analysis. 2017; 139: 148–155.
[27] J. Poplawski, J.T. Wrobel, T. Glinka, Panaxydol, a new polyacetylenic epoxide from Panax ginseng roots. Phytochemistry. 1980; 19: 1539–1541.
[28] Lu H, Li J, Li M, Gong T, Zhang Z. Systemic delivery of alpha-asarone with Kolliphor HS 15 improves its safety and therapeutic effect on asthma. Drug Delivery. 2015; 22: 266–275.
[29] Dong S, Feng S, Chen Y, Chen M, Yang Y, Zhang J, *et al*. Nerve Suture Combined With ADSCs Injection Under Real-Time and Dynamic NIR-II Fluorescence Imaging in Peripheral Nerve Regeneration *in vivo*. Frontiers In Chemistry. 2021; 9: 676928.
[30] Hare GM, Evans PJ, Mackinnon SE, Best TJ, Bain JR, Szalai JP, *et al*.Walking track analysis: a long-term assessment of peripheral nerve recovery. Plastic and Reconstructive Surgery. 1992; 89: 251–258.
[31] Sakuma M, Gorski G, Sheu SH, Lee S, Barrett LB, Singh B, *et al*. Lack of motor recovery after prolonged denervation of the neuromuscular junction is not due to regenerative failure. European Journal of Neuroscience. 2016; 43: 451–462.
[32] Melchart D, Hager S, Albrecht S, Dai J, Weidenhammer W, Teschke R. Herbal. Traditional Chinese Medicine and suspected liver injury: A prospective study. World Journal of Hepatology. 2017; 9: 1141–1157.
[33] Chow HC, So TH, Choi HCW, Lam KO. Literature review of traditional Chinese. medicine herbs-induced liver injury from an oncological perspective with RUCAM. Integrative Cancer Therapies. 2019; 18: 1534735419869479.
[34] Jing J, Teschke R. Traditional Chinese Medicine and Herb-induced Liver Injury: Comparison with Drug-induced Liver Injury. Journal of Clinical and Translational Hepatology. 2018; 6: 57–68.
[35] Vögelin E, Baker JM, Gates J, Dixit V, Constantinescu MA, Jones NF. Effects of local continuous release of brain derived neurotrophic factor (BDNF) on peripheral nerve regeneration in a rat model. Experimental Neurology. 2006; 199: 348–353.
[36] Chen P, Piao X, Bonaldo P. Role of macrophages in Wallerian degeneration and axonal regeneration after peripheral nerve injury. Acta Neuropathologica. 2015; 130: 605–618.
[37] Painter MW, Brosius Lutz A, Cheng YC, Latremoliere A, Duong K, Miller CM, *et al*. Diminished Schwann cell repair responses underlie age-associated impaired axonal regeneration. Neuron. 2014; 83: 331–343.
[38] Sacchetti M, Lambiase A. Neurotrophic factors and corneal nerve regeneration. Neural Regeneration Research. 2017; 12: 1220–1224.
[39] Guo W, Nagappan G, Lu B. Differential effects of transient and sustained activation of BDNF-TrkB signaling. Developmental Neurobiology. 2018; 78: 647–659.
[40] Suzuki A, Matsuura D, Kanatani H, Yano S, Tsunakawa M, Matsuyama S, *et al*. Inhibitory effects of polyacetylene compounds from panax ginseng on neurotrophin receptor-mediated hair growth. Biological and Pharmaceutical Bulletin. 2017; 40: 1784–1788.
[41] Jeon SW, Kim YK. Neuroinflammation and cytokine abnormality in major depression: Cause or consequence in that illness? World Journal of Psychiatry. 2016; 6: 283–293.
[42] Zhang J, Ding L, Wang B, Ren G, Sun A, Deng C, *et al*. Notoginsenoside R1 attenuates experimental inflammatory bowel disease via pregnane X receptor activation. Journal of Pharmacology and Experimental Therapeutics. 2015; 352: 315–324.
[43] Zheng X, Liang Y, Kang A, Ma SJ, Xing L, Zhou YY, *et al*. Peripheral immunomodulation with ginsenoside Rg1 ameliorates neuroinflammation-induced behavioral deficits in rats. Neuroscience 2014; 256: 210–222.
[44] Hou QL, Wang Y, Li YB, Hu XL, Wang S.L. Protective effect of notoginsenoside R1 on neuron injury induced by OGD/R through ATF6/Akt signaling pathway. China Journal of Chinese Materia Medica. 2017; 42: 1167–1174. (In Chinese)
[45] Li W, Ling S, Yang Y, Hu Z, Davies H, Fang M. Systematic hypothesis for post-stroke depression caused inflammation and neurotransmission and resultant on possible treatments. Neuroendocrinology Letters. 2014; 35: 104–109.
[46] Yang X, Yang S, Hong C, Yu W, Guonian W. Panax Notoginseng Saponins attenuates sevofluraneinduced nerve cell injury by modulating AKT signaling pathway. Molecular Medicine Reports. 2017; 16: 7829–7834.
[47] Lee IS, Kang KS, Kim SY. Panax ginseng pharmacopuncture: current status of the research and future challenges. Biomolecules. 2019; 10: 33.
[48] Razgonova MP, Veselov VV, Zakharenko AM, Golokhvast KS, Nosyrev AE, Cravotto G, *et al*. Panax ginseng components and the pathogenesis of Alzheimer's disease (Review). Molecular

Medicine Reports. 2019; 19: 2975–2998.
[49] Im DS. Pro-Resolving Effect of ginsenosides as an anti-inflammatory mechanism of Panax ginseng. Biomolecules. 2020; 10: 444.
[50] Gordon T, Borschel GH. The use of the rat as a model for studying peripheral nerve regeneration and sprouting after complete and partial nerve injuries. Experimental Neurology. 2017; 287: 331–347.
[51] Gordon T. Neurotrophic factor expression in denervated motor and sensory Schwann cells: relevance to specificity of peripheral nerve regeneration. Experimental Neurology. 2014; 254: 99–108.
[52] Grosheva M, Nohroudi K, Schwarz A, Rink S, Bendella H, Sarikcioglu L, *et al*. Comparison of trophic factors' expression between paralyzed and recovering muscles after facial nerve injury. A quantitative analysis in time course. Experimental Neurology. 2016; 279: 137–148.
[53] Ma CH, Omura T, Cobos EJ, Latrémolière A, Ghasemlou N, Brenner GJ, *et al*. Accelerating axonal growth promotes motor recovery after peripheral nerve injury in mice. Journal of Clinical Investigation. 2011; 121: 4332–4347.
[54] Khodorova A, Nicol GD, Strichartz G. The TrkA receptor mediates experimental thermal hyperalgesia produced by nerve growth factor: modulation by the p75 neurotrophin receptor. Neuroscience. 2017; 340: 384–397.
[55] Jiao Y, Palmgren B, Novozhilova E, Johansson UE, Spieles-Engemann AL, Kale A, *et al*. BDNF increases survival and neuronal differentiation of human neural precursor cells co-transplanted with a nanofiber gel to the auditory nerve in a rat model of neuronal damage. BioMed Research International. 2014; 2014: 356415.
[56] Wang X, Zhang L, Zhan Y, Li D, Zhang Y, Wang G, *et al*. Contribution of BDNF/TrkB signalling in the rACC to the development of pain-related aversion via activation of ERK in rats with spared nerve injury. Brain Research. 2017; 1671: 111–120.
[57] Zhang Y, Zhao J, Wang J, Jiao X. Brain-derived neurotrophic factor inhibits phenylalanine-induced neuronal apoptosis by preventing RhoA pathway activation. Neurochemical Research. 2010; 35: 480–486.
[58] Eberhardt KA, Irintchev A, Al-Majed AA, Simova O, Brushart TM, Gordon T, *et al*. BDNF/TrkB signaling regulates HNK-1 carbohydrate expression in regenerating motor nerves and promotes functional recovery after peripheral nerve repair. Experimental Neurology. 2006; 198: 500–510.
[59] Roux PP, Barker PA. Neurotrophin signaling through the p75 neurotrophin receptor. Progress in Neurobiology. 2002; 67: 203–233.
[60] Meeker RB, Williams KS. The p75 neurotrophin receptor: at the crossroad of neural repair and death. Neural Regeneration Research. 2015; 10: 721–725.